

Electronic Supplementary Information

Resonance Plasmonic Coupling: Selective Enhancement of Band Edge Emission over Trap State Emission of CdSe Quantum Dots

Livin Paul,^a Elizabeth Mariam Thomas,^a Akshaya Chemmangat,^a

*Stephen K. Gray,^{*b} K. George Thomas^{*a}*

^aSchool of Chemistry, Indian Institute of Science Education and Research

Thiruvananthapuram (IISER TVM), Vithura, Thiruvananthapuram, 695551, India

^bCenter for Nanoscale Materials, Argonne National Laboratory, Argonne, Illinois 60439,

United States

Sl. No.	Contents	Page No.
ESI 1	Materials	S2
ESI 2	Synthesis and characterization of CdSe QDs	S2
ESI 3	Synthesis and characterization of CdSe/ZnS QDs	S3
ESI 4	Synthesis and characterization of plasmonic nanoparticles	S5
ESI 5	Characterization of silica nanoparticles	S6
ESI 6	Concentration calculation of SiO ₂ NPs	S7
ESI 7	Stability of CdSe bound plasmonic nanoparticles	S8
ESI 8	Inner filter effect corrections	S8
ESI 9	Surface effect correction	S9
ESI 10	Photophysical studies of CdSe QDs on AuNPs	S11
ESI 11	Intensity-based enhancement factor of CdSe QDs on AuNPs	S12
ESI 12	Contribution from excitation and emission rate enhancement to the overall EF	S12
ESI 13	Effect of the plasmonic field on PL lifetime	S14
ESI 14	Photophysical studies of CdSe/ZnS QDs on SiO ₂ NPs	S14
ESI 15	Photophysical studies of CdSe/ZnS QDs on AuNPs	S15
ESI 16	The band edge PL spectral region of QDs in the presence of AuNPs	S16
ESI 17	Intensity-based enhancement factor of CdSe/ZnS QDs (~100 number) on AuNPs	S16
ESI 18	References	S17

ESI 1. Materials

Cadmium oxide (CdO), trioctylphosphine (TOP), trioctylphosphine oxide (TOPO), selenium powder (Se), zinc acetate, oleic acid, octadecene, oleylamine, trioctylamine, L-cysteine, gold(III) chloride trihydrate, trisodium citrate dihydrate, poly(allylamine hydrochloride) (average MW of 17,500), cadmium chloride hemipentahydrate ($\text{CdCl}_2 \cdot 2.5\text{H}_2\text{O}$), mercaptosuccinic acid (MSA), and selenium dioxide (SeO_2) from Sigma Aldrich and sodium chloride and potassium hydroxide from Merck, tetradecylphosphonic acid (TDPA) from Alfa Aesar, and HPLC grade solvents (hexane, methanol, isopropanol, and acetone) from Spectrochem are used as received.

ESI 2. Synthesis and characterization of CdSe QDs

Mercaptosuccinic acid (MSA) capped CdSe QDs are synthesized by following a reported procedure¹ with a slight modification. Cd-MSA complex is prepared by mixing $\text{CdCl}_2 \cdot 2.5\text{H}_2\text{O}$ (2 mmol) and MSA (3.2 mmol) in deionized water (50 mL) in a three-necked round bottom (RB) flask. The pH of the solution is adjusted using NaOH (1 M) solution to 11.8. After attaining a temperature of 60 °C, ascorbic acid (20 mM) and SeO_2 (0.2 mmol) are added under vigorous stirring, and the pH of the reaction mixture is maintained at 11.8 using NaOH (1 M) solution. The reaction mixture is refluxed for 5 h at 100 °C. The CdSe QDs are purified by precipitation with acetone to remove the excess ligands and the starting materials. The purified CdSe QDs are stored in double distilled water for further studies.

The first excitonic peak of CdSe QDs in the absorption spectra, corresponding to the band edge excitation, is observed at 481 nm (blue trace in Fig. 2B). The concentration of CdSe QDs is estimated by absorption spectroscopic studies using the reported procedure² (ϵ at 481 nm = $1.81 \times 10^6 \text{ M}^{-1}\text{cm}^{-1}$). The emission spectrum shows two distinct bands at 506 nm and 675 nm corresponding to band edge and trap state emission, respectively (red trace in Fig. 2B). The transmission electron microscopy image of CdSe QDs is presented in Fig. 1F. The

photoluminescence (PL) quantum yield (ϕ_{PL}) of CdSe QDs in water, in the entire spectral window, is estimated using absolute and relative methods. Coumarin 153 in ethanol is used as the reference ($\phi_{\text{PL}} = 0.544$)³ for the relative method. The sample and reference are excited at 400 nm, keeping their optical density matched (0.06). The ϕ_{PL} of CdSe QDs in water, estimated by absolute and relative methods, is the same (0.09 ± 0.001). The CdSe QDs follow a triexponential decay with an intensity-weighted average lifetime (τ_{avg}) of 35.5 ns (black trace in Fig. 4E). The surface charge of MSA-capped CdSe QDs is estimated using zeta-potential (ζ -potential) studies and the value is found to be -30.9 mV shown in Fig. 2E (black trace).

ESI 3. Synthesis and characterization of CdSe/ZnS QDs

CdSe QDs, capped with tetradecylphosphonic acid (TDPA) and trioctylphosphine oxide (TOPO) are synthesized by following a reported procedure.⁴ Cd-TDPA complex is first synthesized by heating CdO (0.40 mmol) as the cadmium precursor, with TDPA (0.80 mmol) and TOPO (6.46 mmol) at 300 °C in an RB flask kept under nitrogen. Selenium powder (0.4 mmol) in trioctylphosphine (2.24 mmol) is used as the selenium precursor and injected into the above solution, maintaining the temperature. The required size of CdSe QDs is achieved by controlling the growth temperature and duration of the reaction. The reaction is arrested by immediate cooling of the reaction mixture by the removal of the heating source and the addition of toluene (5 mL) using a syringe at 100 °C. The formed CdSe QDs are purified by precipitating the sample using a mixture (1:4) of methanol and acetone. The solid residue is separated by centrifugation, which allows the removal of starting materials and the excess ligands as the supernatant solution. The solid residue is then dissolved in hexane and centrifuged to remove solid impurities. The supernatant solution, which contains CdSe QDs is stored in hexane for further studies.

Overcoating of ZnS on CdSe QDs is carried out by following a reported procedure⁴ with slight modifications. First, the concentration of CdSe QDs is estimated using electronic spectroscopic

studies (ϵ at 540 nm = $1.79 \times 10^5 \text{ M}^{-1}\text{cm}^{-1}$) by following a reported procedure.⁵ Zinc oleate and octanethiol are used as the zinc and sulfur precursors, respectively. CdSe QDs (30 nmol) in hexane (200-400 μL) is added to a mixture of trioctylamine (1 mL) and octadecene (1 mL), and degassed for 1 h at 120 °C under nitrogen. Maintaining the temperature, zinc oleate (35.4 μmol) and octanethiol (53.1 μmol) are added to the reaction mixture and heated to 310 °C for 5 min. The formed core-shell QDs are dissolved in toluene, precipitated with methanol, and redispersed in toluene.

For the phase transfer of long alkyl chain ligands capped CdSe/ZnS QDs from organic medium to aqueous medium, a precipitation method is adopted.⁶ The phase transferred CdSe/ZnS QDs in water are characterized using spectroscopic and microscopic methods. The TEM image of CdSe/ZnS QDs is presented in Fig. 1G. From the absorption and PL studies, it is found that the first excitonic band in the absorption spectrum of CdSe/ZnS QDs peaks at 522 nm, and the emission maximum at 541 nm (Fig. S1A and Fig. 1B). The concentration of QDs is calculated using absorption spectroscopic studies (ϵ at 522 nm = $1.66 \times 10^5 \text{ M}^{-1}\text{cm}^{-1}$) by following a reported procedure.⁵ The surface charge of L-cysteine capped CdSe/ZnS QDs is negative with a ζ -potential value of -28.0 mV (Fig. S1B). The ϕ_{PL} of CdSe/ZnS QDs in water is estimated as 0.11 using the relative method. Coumarin 153 in ethanol is used as the reference ($\phi_{\text{PL}} = 0.544$).³ The sample and reference are excited at 375 nm, keeping the optical density same (0.05).

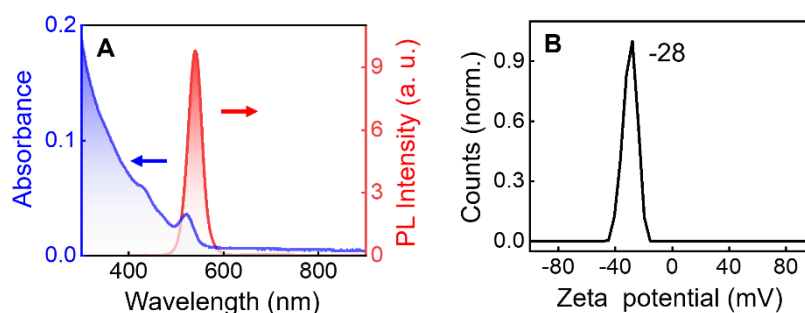


Fig. S1 (A) Absorption spectrum (blue trace), photoluminescence spectrum (red trace), and (B) zeta potential distribution of CdSe/ZnS QDs in water.

ESI 4. Synthesis and characterization of plasmonic nanoparticles

For the synthesis of Au nanoparticles, a kinetically controlled seed-mediated method is adopted.⁷ The Au nanoparticle seeds are synthesized in solution by reducing HAuCl_4 using trisodium citrate dihydrate (TSC) as the reducing agent. The synthesis is carried out in three steps.

In the first step (Step 1), an aqueous solution of TSC (2.2 mM; 150 mL) is kept at 100 °C for 15 min in an RB flask, followed by the addition of HAuCl_4 (25 mM; 1 mL) to this solution. A uniform growth of Au nanoparticle seeds is achieved by keeping the reaction conditions constant for around 15–20 min. The formation of Au nanoparticles of larger size is achieved by stepwise reducing HAuCl_4 by TSC on the surface of previously synthesized seeds by keeping the solution at 90 °C. In step 2, HAuCl_4 (25 mM; 1 mL) is added twice to the reaction mixture at an interval of 30 min, maintaining the temperature at 90 °C. After the second addition, the temperature of the solution is maintained for another 30 min to ensure the completion of the reaction. Subsequently, 55 mL of the reaction mixture is removed from the RB flask. In the third step, double-distilled H_2O (53 mL) and TSC (60 mM; 2 mL) are added to the reaction vessel, and the temperature is allowed to reach 90 °C. After that, Steps 2 and 3 are repeated till the desired size for the nanoparticle is obtained. The solution is centrifuged at 6500 rpm for 30 min to remove the unreacted ligands and Au nanoparticles of smaller dimensions. The residue obtained is dispersed in double-distilled water and stored for further

studies.

The PAH-coated Au NPs are characterized using TEM (Fig. 1D,E, and Fig. S2), UV-vis absorption spectroscopy (Fig. 1C), and zeta-potential measurements (Fig. 1J). The coating of PAH layer on gold nanoparticles is established based on the TEM and zeta-potential studies. It can be seen from the histogram of TEM images that the diameter of the Au core is ~31 nm (Fig. 1H), and the thickness of the polymer shell on the Au nanoparticle is ~1.3 nm (Fig. 1I). The concentration of AuNPs is estimated based on absorption studies by following a reported procedure⁸ (ϵ at 527 nm = $3.92 \times 10^9 \text{ M}^{-1}\text{cm}^{-1}$).

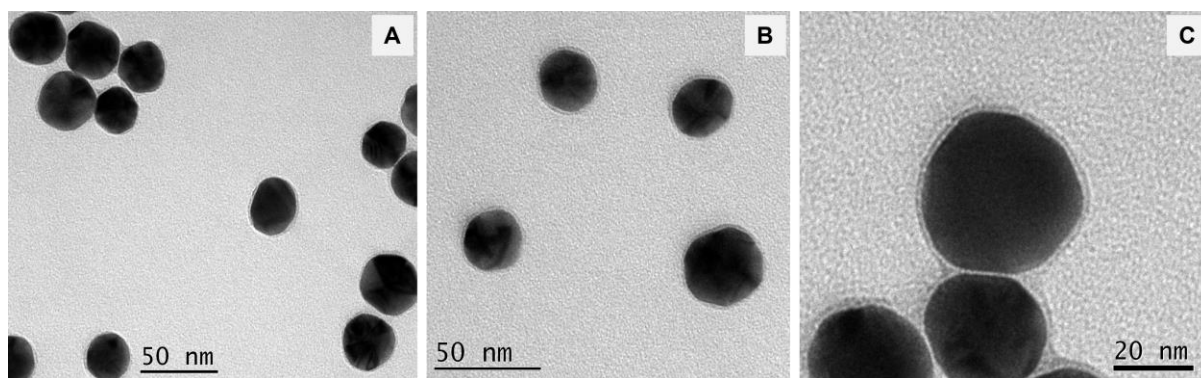


Fig. S2 (A-C) The TEM images of the PAH-coated Au nanoparticles at different magnifications.

ESI 5. Characterization of silica nanoparticles

From the TEM analysis, it is clear that SiO₂ NPs are spherical in shape, and the average size is ~161 nm (Fig. S3A). The concentration of SiO₂ NPs in the stock solution is calculated using inductively coupled plasma-optical emission spectroscopy (ICP-OES). The extinction spectrum of SiO₂ NPs does not possess any distinct peaks (Fig. S3B), which is its characteristic feature. The surface charge of PAH-capped SiO₂ NPs is found positive with a ζ -potential value

of +38.0 mV (Fig. S3C).

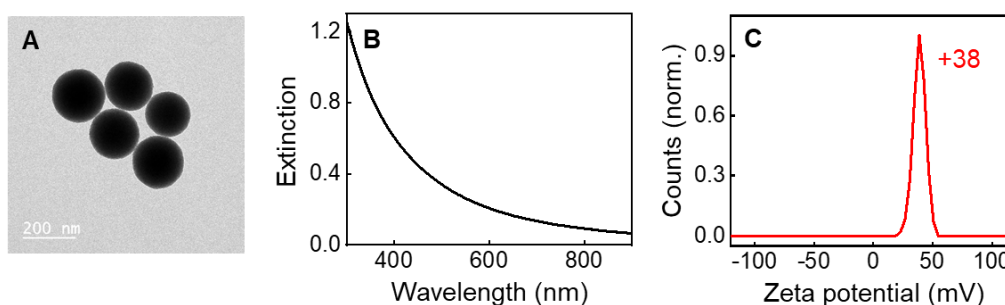


Fig. S3 (A) TEM image, (B) extinction spectrum, and (C) zeta potential distribution of SiO₂ NPs.

ESI 6. Concentration calculation of SiO₂ NPs

The concentration of SiO₂ NPs is estimated using ICP-OES and TEM analysis as listed below.

The diameter (d) of the SiO₂ particle obtained from TEM analysis is 161 nm.

$$\text{Density of SiO}_2 \text{ NP} = 2.0 \text{ g/cm}^3$$

$$\begin{aligned} \text{Volume of a spherical SiO}_2 \text{ NP} &= \frac{4}{3} \pi (80.5 \text{ nm})^3 \\ &= 2.18 \times 10^6 \text{ nm}^3 \end{aligned}$$

$$\text{Mass of one SiO}_2 \text{ NP} = 4.36 \times 10^{-15} \text{ g}$$

The mass of SiO₂ NPs in 5 mL of water, obtained by ICP-OES analysis, is 3.89 mg

$$\text{Number of SiO}_2 \text{ NPs in 5 mL of water} = 0.892 \times 10^{12}$$

(mass of SiO₂ NPs/mass of one SiO₂ NP)

$$\begin{aligned} \text{Number of moles of SiO}_2 \text{ NPs in 5 mL} &= 0.892 \times 10^{12} / 6.023 \times 10^{23} \\ &= 0.148 \times 10^{-11} \text{ mol} \end{aligned}$$

$$\text{Molar concentration of SiO}_2 \text{ NPs} = 0.29 \times 10^{-9} \text{ M}$$

(moles per unit concentration)

ESI 7. Stability of CdSe bound plasmonic nanoparticles

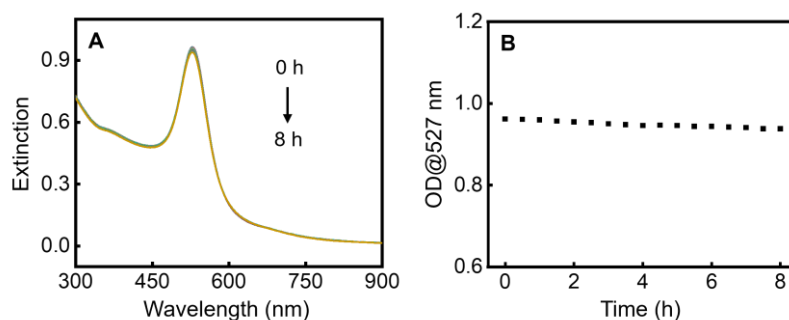


Fig. S4 (A) Extinction spectrum of CdSe QDs bound on AuNPs recorded for 8 h at a time interval of 30 min. (B) The optical density of the hybrid systems monitored at the extinction maximum at 527 nm for 8 h.

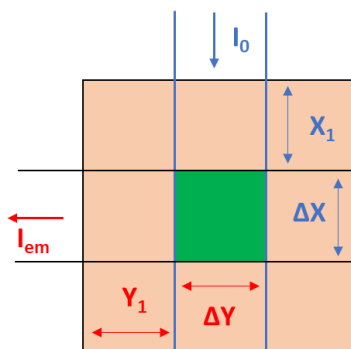
Note: The addition of concentrated QDs to the AuNPs solution often results in aggregation due to rapid QD binding, leading to a high density of negatively charged CdSe QDs localized within a small volume. Adding a small (~1-2 μL) volume of a highly concentrated QD stock solution causes aggregation. Instead, it is advisable to add a slightly larger volume (~10-20 μL) of a more dilute stock solution.

ESI 8. Inner filter effect corrections

The photoluminescence spectra of QDs in the presence of the plasmonic nanoparticles are corrected for the inner filter effects (IFE) by following the cell shift method.⁹

In the case of PL studies of a hybrid system (QD bound to a plasmonic nanoparticle), IFEs arise due to the scavenging of excitation light (primary IFE) and the emission light from the QDs (secondary IFE) by the AuNPs. As a result, the observed emission intensity will be less than the actual intensity and it is essential to use the correction factor (CF) in the PL spectrum of hybrid systems. All the hybrid system studies are carried out in a single cuvette and we have accounted for both primary and secondary IFEs correction by following a cell shift method as reported in the literature.^{9, 10} The details about the correction factors and various parameters used are given below.

Scheme S1. The dimensions of excitation and emission beam passing through the cuvette.



The orange box shown in Scheme S1 represents the cross-sectional view of a cuvette. The green-colored region in the center of the cuvette represents the region from which the emitted light is detected by the detector, termed the fluorescence observation field (FOF).¹¹ The reduction in the intensity of the excitation beam on passing through X_1 before reaching the FOF is termed the primary inner filter effect (IFE 1). Similarly, the reduction in PL intensity due to the reabsorption of the emitted light on passing through the Y_1 region is termed the secondary inner filter effect (IFE 2). The reduction in PL intensity of the emitter due to IFE 1 and IFE 2 in a single cuvette can be accounted together by using the eqn S1,

$$IFE = \frac{2.303 A_{ex}(\Delta x)10^{A_{ex}x_1}}{1-10^{-A_{ex}\Delta x}} \frac{2.303 A_{em}(\Delta y)10^{A_{em}y_1}}{1-10^{-A_{em}\Delta y}}, \quad (S1)$$

where A_{ex} and A_{em} are the optical densities of the sample at the excitation and the emission wavelengths, respectively. Estimation of the FOF dimensions, Δx and Δy , is achieved using the cell-shift method.⁹ All the PL spectra of the QDs in the presence of the AuNPs presented in this study are corrected by multiplying the observed emission spectrum with the IFE (eqn S1).

ESI 9. Surface effect correction

CdSe QDs when bound on PAH-coated gold nanoparticles, variation of PL due to surface effects (SE) can also occur along with plasmonic field effects.

In order to quantify the change in PL, due to the binding of QDs on the surface of PAH-coated gold nanoparticles, a control experiment is carried out using PAH-coated silica nanoparticle (SiO_2 NPs) wherein plasmonic effects are not observed.

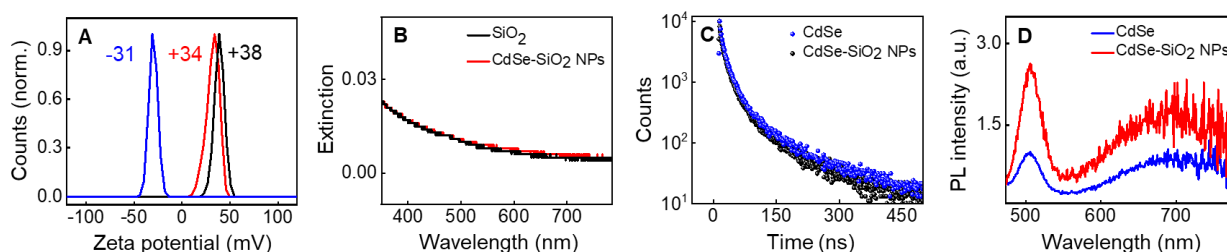


Fig. S5 (A) Zeta potential distribution of CdSe QDs (blue trace), and SiO_2 NPs before (black trace) and after (red trace) the addition of CdSe QDs. (B) Extinction spectrum of SiO_2 NPs before (black trace) and after (red trace) the addition of CdSe QDs. (C) PL decay profile of CdSe QDs before (blue trace) and after the addition of SiO_2 NPs (black trace). (D) PL spectrum of CdSe QDs before (blue trace) and after (red trace) the addition of SiO_2 NPs.

The binding of CdSe QDs on SiO_2 NPs is confirmed by following zeta potential studies (Fig. S5A). The extinction spectrum of SiO_2 NPs in the absence and presence of CdSe QDs remains unchanged (Fig. S5B). The PL lifetime of CdSe QDs in the absence and presence of SiO_2 NPs remains more or less unchanged (Fig. S5C) ruling out the possibility of various photophysical processes such as energy and electron transfer when QDs are bound on SiO_2 NPs. On the addition of CdSe QDs to the SiO_2 NPs, ~ 2.3 -fold enhancement in PL intensity is observed in the entire spectral range of 475–780 nm (Fig. S5D). Thus, a surface effect correction term is introduced to account for the PL variation influenced by the surface, namely PAH. The IFE-corrected PL spectrum of the QDs is further divided by the SE correction factor (2.3) in the entire spectral region (eqn 1 in the main text).

Theoretically, we have calculated the radiative enhancement factor of QDs when bound on the SiO_2 NPs having a refractive index of 1.5, and no changes are observed in comparison with the free emitter. In the experimental studies, the positive charge is provided to SiO_2 NPs by the functional groups on their surface which may be responsible for the surface effects.

ESI 10. Photophysical studies of CdSe QDs on AuNPs

Two independent sets of experiments are carried out by binding CdSe QDs on AuNPs. The PL intensity of CdSe QDs in the absence and presence of AuNPs are presented along with IFE and SE corrected spectrum.

Set 1

Results obtained from Set 1 is presented in Fig. 4 in the main text.

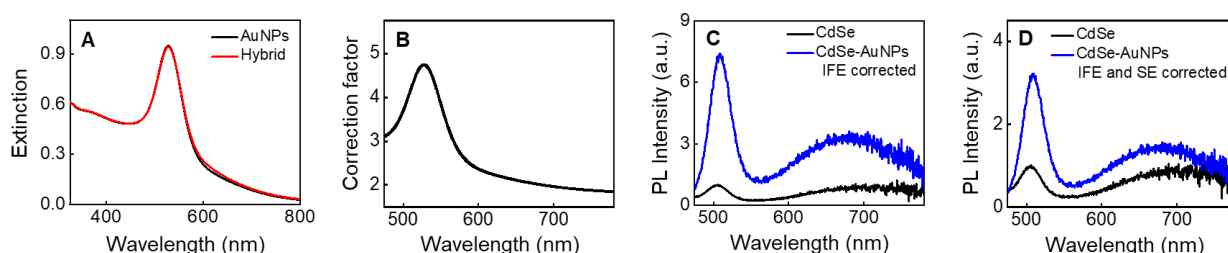


Fig. S6 Selective enhancement of band edge emission of CdSe (Set 1): (A) Extinction spectra of AuNPs before (black trace) and after (red trace) the addition of CdSe QDs. (B) Correction factor used for the IFE correction. (C,D) PL spectrum of CdSe QDs (black trace) and hybrid system (blue trace) after (C) IFE correction and (D) IFE and SE correction.

Set 2

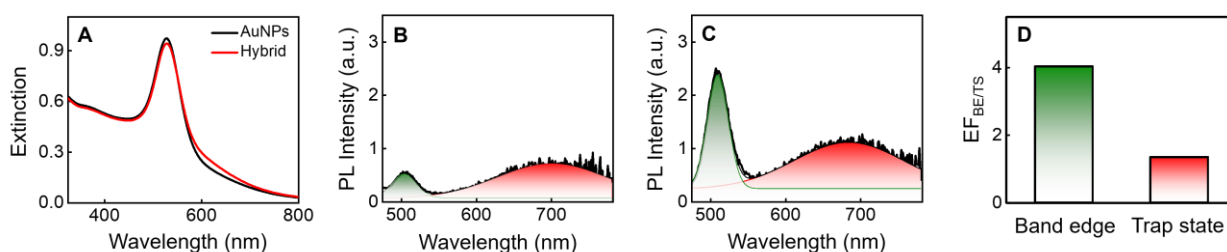


Fig. S7 Selective enhancement of band edge emission of CdSe (Set 2): (A) Extinction spectrum of AuNPs before (black trace) and after (red trace) the addition of CdSe QDs. PL spectrum of CdSe QDs before (B) and after (C) the addition of AuNPs. (D) Area-based PL enhancement corresponding to the band edge (green shaded region) and trap state (red shaded region) are shown.

ESI 11. Intensity-based enhancement factor of CdSe QDs on AuNPs

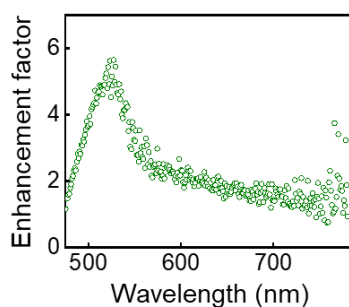


Fig. S8 Experimentally calculated intensity-based PL enhancement factor (EF_{λ}) of CdSe QDs bound on AuNPs in the spectral window of 475–780 nm of Set 2. EF_{λ} of Set 1 is shown in Fig. 4F.

ESI 12. Contribution from excitation and emission rate enhancement to the overall EF

Plasmon-assisted emission enhancement of an emitter has contributions from both the excitation and emission rate enhancement. On-resonance coupling of the plasmon band with the band edge emission of CdSe QDs due to the spectral overlap is responsible for the emission rate enhancement, whereas the trap state emission remains in an off-resonance condition. In contrast, spectral overlap between the absorption spectrum of the emitter and the extinction spectrum of the plasmonic material at the excitation wavelength is responsible for the excitation rate enhancement. Due to the unavoidable spectral overlap between the absorption spectrum of the QDs with the extinction spectrum of the AuNPs at the excitation wavelength, a small excitation rate enhancement occurs.

Excitation rate enhancement is only influenced by the excitation wavelength, and hence the enhancement factor will remain constant across all emission wavelengths. In Fig. S9, the green vertical line corresponds to the excitation wavelength. It can be seen that the spectral overlap between the trap state emission of CdSe QDs with the extinction spectrum of AuNPs is minimal at the blue-shaded region (700-780 nm). Thus the observed PL enhancement at higher emission wavelengths is majorly due to the excitation rate enhancement. We calculated the enhancement of emission, in the presence of AuNPs, in the blue-shaded region as 1.34.

However, the emission rate enhancement will vary with the wavelength, due to its dependence on the spectral overlap. The contribution of emission rate enhancement (from total emission enhancement) at each wavelength is calculated by dividing the EF_{λ} with the excitation rate enhancement factor (1.34) and spectrum is constructed (Fig. S10).

Similarly, we theoretically calculated the excitation enhancement factor and radiative rate enhancement factor. The theoretically calculated excitation enhancement, F_{ex} , at the excitation wavelength (400 nm) is found to be 1.8 times and it is in agreement with the experimental calculations (1.34). The theoretically calculated radiative rate enhancement factor of QDs at the emission wavelengths is shown in Fig. 4G. The calculated radiative rate enhancement factor (Fig. 4G) shows a good spectral overlap with EF_{λ} presented in Fig. 4F.

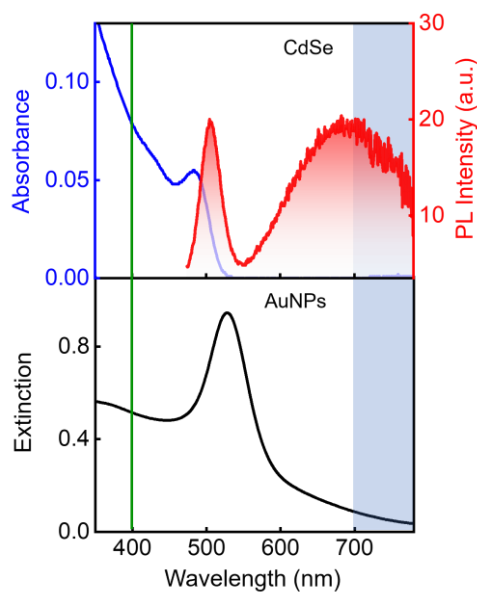


Fig. S9 Absorption (blue trace) and emission (red trace) spectra of CdSe QDs, and extinction spectrum (black trace) of AuNPs. Note: The emission spectrum is collected by exciting the sample at 400 nm, shown by the green line. The blue strip in the stacked plot represents the overlap between the emission spectrum of CdSe QDs and the extinction spectrum of AuNPs.

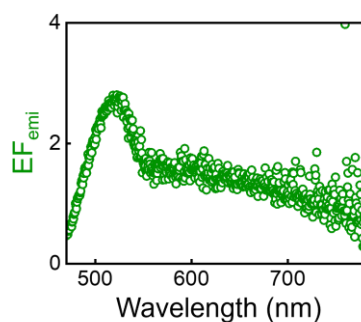


Fig. S10 Experimental PL enhancement factor of CdSe QDs bound on AuNPs in the spectral window of 475–780 nm, calculated after removing the contribution from the excitation rate enhancement.

ESI 13. Effect of the plasmonic field on PL lifetime

The PL decay curve of the bare CdSe QDs is fitted using the triexponential function. The triexponential decay kinetics involves three recombination pathways: emission due to the recombination of (i) τ_1 - hole trap, (ii) τ_2 - band edge exciton, and (iii) τ_3 - electronic trap states.¹²

Table S1. The PL lifetime of CdSe QDs at 506 nm in the absence and presence of plasmonic nanoparticles.

Lifetime components	In the absence of plasmonic field (ns)	In the presence of plasmonic field (ns)
τ_1	4.58	1.15
τ_2	20.01	8.39
τ_3	98.75	42.16

ESI 14. Photophysical studies of CdSe/ZnS QDs on SiO₂ NPs

In order to quantify the change in PL, due to the binding of QDs on the surface of PAH-coated gold nanoparticles, a control experiment is carried out using PAH-coated silica nanoparticles wherein plasmonic effects are not observed. The binding of CdSe/ZnS QDs on SiO₂ NPs is confirmed by following zeta potential studies (Fig. S11A). The extinction spectrum of SiO₂ NPs in the absence and presence of CdSe/ZnS QDs remains unchanged (Fig. S11B). By the addition of CdSe/ZnS QDs to the SiO₂ NPs, an average of 2-fold enhancement in PL intensity is observed (Fig. S11C). To account for the enhancement in the PL spectrum in the absence of

the plasmonic field, a surface effect correction term is introduced. The IFE-corrected PL spectrum of the QDs is further divided by the SE correction factor (2) in the entire spectral region.

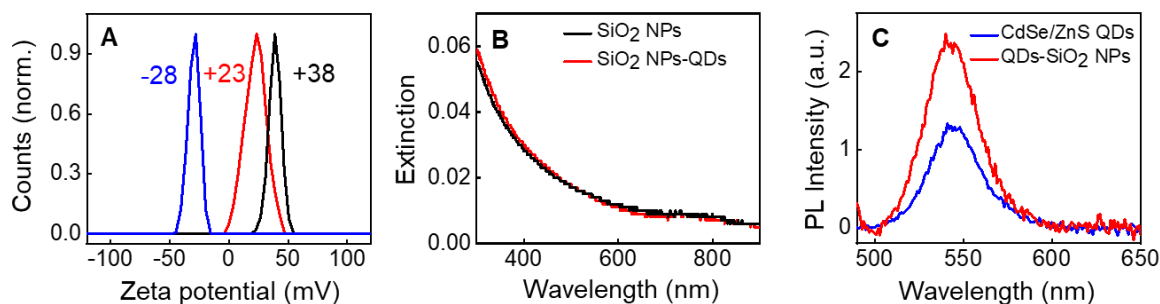


Fig. S11 (A) Zeta potential distribution of CdSe/ZnS QDs (blue trace) and SiO₂ NPs before (black trace) and after (red trace) the addition of CdSe/ZnS QDs. (B) Extinction spectrum of SiO₂ NPs before (black trace) and after (red trace) the addition of CdSe/ZnS QDs. (C) PL spectrum of CdSe/ZnS QDs before (blue trace) and after (red trace) addition of SiO₂ NPs.

ESI 15. Photophysical studies of CdSe/ZnS QDs on AuNPs

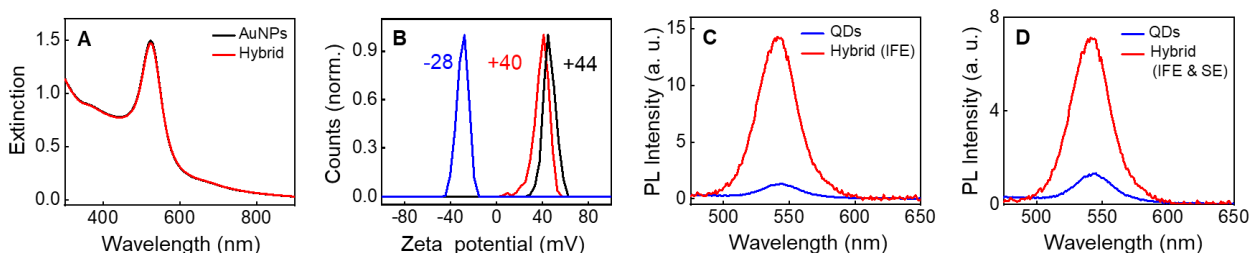


Fig. S12 (A-D) Photophysical studies of CdSe/ZnS QDs (~10 number) on AuNPs. (A) Extinction spectrum of AuNPs before (black trace) and after (red trace) the addition of CdSe/ZnS QDs. (B) Zeta potential distribution of CdSe/ZnS QDs (blue trace) and AuNPs before (black trace) and after (red trace) the addition of CdSe/ZnS QDs. (C,D) PL spectrum of CdSe/ZnS QDs (blue trace) and hybrid system (red trace) with IFE and SE corrections; (C) IFE corrected and (D) IFE and SE corrected.

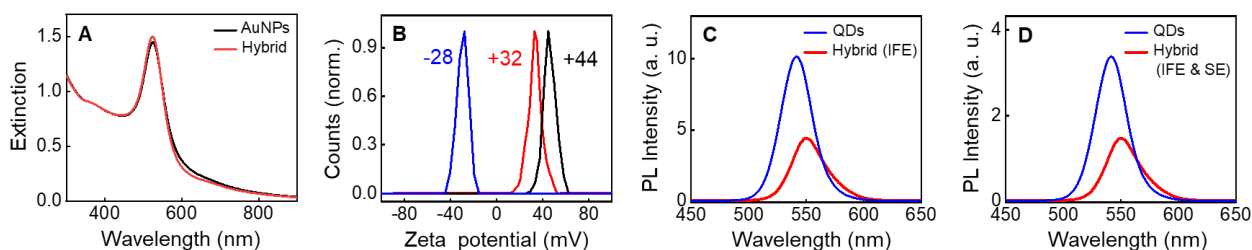


Fig. S13 (A-D) Photophysical studies of CdSe/ZnS QDs (~100 number) on AuNPs. (A) Extinction spectrum of AuNPs before (black trace) and after (red trace) the addition of CdSe/ZnS QDs. (B) Zeta potential distribution of CdSe/ZnS QDs (blue trace) and AuNPs before (black trace) and after (red trace) the addition of CdSe/ZnS QDs. (C,D) PL spectrum of CdSe/ZnS QDs (blue trace) and hybrid system (red trace) with IFE and SE corrections; (C) IFE corrected and (D) IFE and SE corrected.

ESI 16. The band edge PL spectral region of QDs in the presence of AuNPs

Upon binding QDs to AuNPs, it can be seen that the band edge emission maximum remains more or less unchanged for (i) CdSe QDs and (ii) CdSe/ZnS QDs (1:10). However the band edge emission maximum shifted by 9 nm for CdSe/ZnS QDs (1:100).

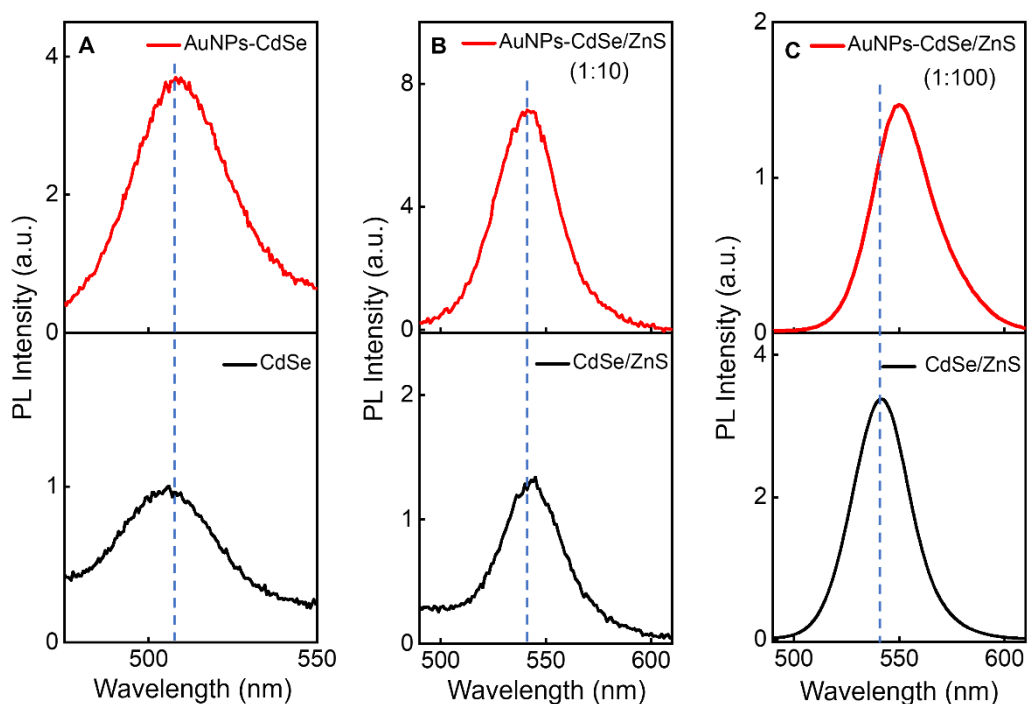


Fig. S14 (A) The PL spectrum of CdSe QDs (452 pM) in the absence (black trace) and the presence (red trace) of AuNPs (207 pM) in the spectral window of 475-550 nm. (B) The PL spectrum of CdSe/ZnS QDs (3.72 nM) in the absence (black trace) and the presence (red trace) of AuNPs (340 pM) in the spectral window of 490-610 nm. (C) The PL spectrum of CdSe/ZnS QDs (38 nM) in the absence (black trace) and the presence (red trace) of AuNPs (340 pM) in the spectral window of 490-610 nm.

ESI 17. Intensity-based enhancement factor of CdSe/ZnS QDs (~100 number) on AuNPs

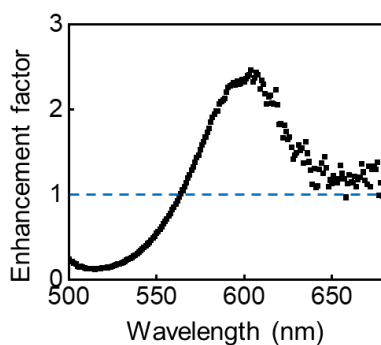


Fig. S15 Experimentally calculated intensity-based PL enhancement factor (EF_{λ}) of CdSe/ZnS QDs bound on AuNPs in the spectral window of 500–680 nm.

ESI 18. References

1. Y. Wang, M. Yu, K. Yang, J. Lu and L. Chen, *Luminescence*, 2015, **30**, 1375-1379.
2. J. Li, J. Chen, Y. Shen and X. Peng, *Nano Res.*, 2018, **11**, 3991-4004.
3. K. Rurack and M. Spieles, *Anal. Chem.*, 2011, **83**, 1232-1242.
4. K. Boldt, N. Kirkwood, G. A. Beane and P. Mulvaney, *Chem. Mater.*, 2013, **25**, 4731-4738.
5. J. Jasieniak, L. Smith, J. van Embden, P. Mulvaney and M. Califano, *J. Phys. Chem. C*, 2009, **113**, 19468-19474.
6. E. M. Thomas, C. L. Cortes, L. Paul, S. K. Gray and K. G. Thomas, *Phys. Chem. Chem. Phys.*, 2022, **24**, 17250-17262.
7. N. G. Bastús, J. Comenge and V. Puentes, *Langmuir*, 2011, **27**, 11098-11105.
8. J. R. G. Navarro and M. H. V. Werts, *Analyst*, 2013, **138**, 583-592.
9. Q. Gu and J. E. Kenny, *Anal. Chem.*, 2009, **81**, 420-426.
10. B. C. MacDonald, S. J. Lvin and H. Patterson, *Anal. Chim. Acta*, 1997, **338**, 155-162.
11. S. K. Panigrahi and A. K. Mishra, *J. Photochem. Photobiol., C*, 2019, **41**, 100318.
12. A. Thomas, K. Sandeep, S. M. Somasundaran and K. G. Thomas, *ACS Energy Lett.*, 2018, **3**, 2368-2375.